Acta Crystallographica Section F
Structural Biology and Crystallization Communications
ISSN 1744-3091

Ayala Lampel,[a] Oren Yaniv,[a,b] Or Berger,[a] Eran Bacharach,[c] Ehud Gazit[a] and Felix Frolow[a,b]*

[a]Molecular Microbiology and Biotechnology, Tel Aviv University, 69978 Tel Aviv, Israel, [b]Daniella Rich Institute for Structural Biology, Tel Aviv University, 69978 Tel Aviv, Israel, and [c]Cell Research and Immunology, Tel Aviv University, 69978 Tel Aviv, Israel

Correspondence e-mail: mbfrolow@post.tau.ac.il

Received 7 March 2013
Accepted 30 April 2013

PDB Reference: carboxy-terminal domain of HIV-1 capsid protein, 4ipy

A triclinic crystal structure of the carboxy-terminal domain of HIV-1 capsid protein with four molecules in the asymmetric unit reveals a novel packing interface

The Gag precursor is the major structural protein of the virion of human immunodeficiency virus-1 (HIV-1). Capsid protein (CA), a cleavage product of Gag, plays an essential role in virus assembly both in Gag-precursor multimerization and in capsid core formation. The carboxy-terminal domain (CTD) of CA contains 20 residues that are highly conserved across retroviruses and constitute the major homology region (MHR). Genetic evidence implies a role for the MHR in interactions between Gag precursors during the assembly of the virus, but the structural basis for this role remains elusive. This paper describes a novel triclinic structure of the HIV-1 CA CTD at 1.6 Å resolution with two canonical dimers of CA CTD in the asymmetric unit. The canonical dimers form a newly identified packing interface where interactions of four conserved MHR residues take place. This is the first structural indication that these MHR residues participate in the putative CTD–CTD interactions. These findings suggest that the molecules forming this novel interface resemble an intermediate structure that participates in the early steps of HIV-1 assembly. This interface may therefore provide a novel target for antiviral drugs.

1. Introduction

During the replication cycle of human immunodeficiency virus-1 (HIV-1), a key event in the formation of an immature noninfectious virus particle is the assembly of the 55 kDa structural polyprotein Gag (Scarlata & Carter, 2003; Adamson & Jones, 2004). To mature into the infectious particle, the nascent virion requires that Gag undergoes proteolytic cleavage. This cleavage, which is brought about by the viral protease, generates several major proteins, including the capsid protein (CA), which self-assembles into the conical core (capsid) structure of the mature virus (Göttlinger, 2001).

CA comprises two independently folded helical domains, the N-terminal domain (NTD) and the C-terminal domain (CTD), connected by a flexible linker. Crystallographers have determined several high-resolution structures of isolated CA domains and of full-length CA (Gitti *et al.*, 1996; Berthet-Colominas *et al.*, 1999; Gamble *et al.*, 1996, 1997; Kelly *et al.*, 2006; Momany *et al.*, 1996; Ternois *et al.*, 2005; Worthylake *et al.*, 1999; Tang *et al.*, 2002; Wong *et al.*, 2008; Pornillos *et al.*, 2009; Byeon *et al.*, 2009; Ganser-Pornillos *et al.*, 2007; the respective PDB entries are 1gds, 1e6j, 1ak4, 1a8o, 2jpr, 1afv, 2buo, 1a43, 1gwp, 2jyp, 3h47, 2kod and 3dik). These structures reveal three different intermolecular interfaces formed by the mature capsid core: the NTD–NTD interface forms hexameric rings (Gamble *et al.*, 1996; Gitti *et al.*, 1996; Li *et al.*, 2000), the NTD–CTD interface stabilizes the hexamer (Lanman *et al.*, 2003, 2004; Ganser-Pornillos *et al.*, 2007; Pornillos *et al.*, 2009) and the CTD–CTD interface connects adjacent hexameric rings (Gamble *et al.*, 1997; Li *et al.*, 2000; Momany *et al.*, 1996).

Despite extensive structural studies of CA, no high-resolution structural data are available for the arrangement of Gag within the shell of the immature particle. It is generally accepted based on genetic studies that the CTD interface of CA, which is important for capsid core formation, also plays a significant role in Gag–Gag

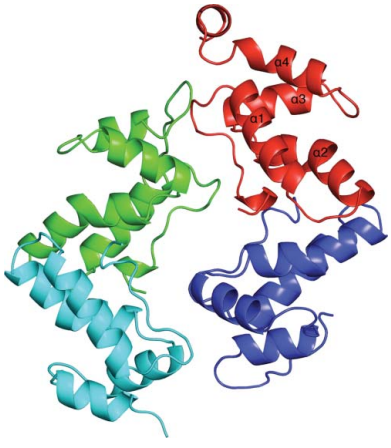

```
HIV-1       (HXB2)  153  I  R  Q  G  P  K  E  P  F  R  D  Y  V  D  R  F  Y  K  T  L  172
HIV-2       (ROD)   287  I  K  Q  G  P  K  E  P  F  Q  S  Y  V  D  R  F  Y  K  S  L  306
SIVmac239           286  V  K  Q  G  P  K  E  P  F  Q  S  Y  V  D  R  F  Y  K  S  L  305
FIV                 280  L  R  Q  G  A  K  E  D  Y  S  S  F  I  D  R  L  F  A  Q  I  299
BIV                 290  I  H  Q  G  P  K  E  P  Y  T  D  F  I  N  R  L  V  A  A  L  309
EIAV                277  I  R  Q  G  A  K  E  P  Y  P  E  F  V  D  R  L  L  S  Q  I  296
```

Figure 1
Alignment of MHR sequences from CA domains of different retroviruses. The alignment was performed with *ClustalW* (Larkin *et al.*, 2007). The conserved Arg154, Pro157, Lys158 and the highly conserved Arg167, which are all relevant to the structure presented in this study, are highlighted in yellow, green, red and cyan, respectively. MHR positions within Gag are indicated for HIV-2 (NP_056837), SIVmac239 (FOLJG3), FIV (NP_040972), BIV (NP_040562) and EIAV (NP_056901); for HIV-1 (NP_579880), MHR positions within CA are indicated. GenBank accession numbers are indicated in parentheses. SIVmac239, simian immunodeficiency virus isolate mac239; FIV, feline immunodeficiency virus; BIV, bovine immunodeficiency virus; EIAV, equine infectious anaemia virus.

interactions. The amino-acid residues Trp184 and Met185, which are located at the dimerization interface of the CA CTD, mediate the formation of the capsid core inside the mature virion. Moreover, these two residues are considered to be important for the assembly of Gag into immature particles, since alanine-substitution mutations at these sites diminish the production of immature particles (von Schwedler *et al.*, 2003; Gamble *et al.*, 1997; Burniston *et al.*, 1999). However, neither the exact structural basis for Gag multimerization nor the assembly mechanism of the immature particle is yet known. It is assumed that in addition to the dimerization interface of the CA CTD, a highly conserved segment within the CA CTD known as the major homology region (MHR) participates in the assembly of the immature particle (Fig. 1). Mutations in this region diminish the assembly of both the immature and the mature particles and abolish infectivity (Borsetti *et al.*, 1998; von Schwedler *et al.*, 2003; Ganser-Pornillos *et al.*, 2004; Chang *et al.*, 2007). Nevertheless, with regard to the assembly of the virus particle, the exact role of the MHR, which to date has not been shown to be involved in the CA CTD dimerization interface, has remained elusive.

Here, we report a newly determined X-ray structure of the CA CTD showing four independent molecules in the asymmetric unit. This structure reveals for the first time a CTD–CTD interface that connects two canonical CTD dimers. The new interface is mediated in part by four conserved amino-acid residues located within the MHR: Arg154, Pro157, Lys158 and Arg167. Lys158 has previously been shown to play a critical role in the assembly of the virus particle *in vivo* and in viral infectivity (Ganser-Pornillos *et al.*, 2004; von Schwedler *et al.*, 2003; Chang *et al.*, 2007). Arg154 has been shown to mediate CA dimerization *in vitro* (del Alamo *et al.*, 2003) and the Arg167Ala mutation has been reported to decrease virus formation *in vivo* (Mammano *et al.*, 1994). We suggest that these four conserved MHR residues participate in CA oligomerization. We present a model which we believe represents a structural intermediate that participates in the assembly of the immature virus particle.

2. Materials and methods

2.1. Protein expression and purification

The expression vector for HIV-1 CA CTD was kindly provided by Professor W. I. Sundquist (University of Utah). *Escherichia coli* BL21 (DE3) cells harbouring the expression plasmid were grown under aerobic conditions at 310 K until the culture reached an A_{600} of 0.6. The recombinant CA CTD (molecular mass 9650 Da) was purified by cation-exchange chromatography (SP Sepharose, GE Healthcare) followed by gel filtration (Superdex 75, GE Healthcare) using an ÄKTAprime system (GE Healthcare). Analysis of the gel-filtration profile (Fig. 2) revealed that the apparent molecular mass is 44 184 Da, indicating an oligomeric association state of a tetramer or pentamer. The protocol described above yielded 8 mg protein from 4 l of bacterial culture.

2.2. Crystallization

Crystals of CA CTD were grown at 293 K by the hanging-drop vapour-diffusion method (McPherson, 1982) using the PEG/Ion crystallization screen (Hampton Research). Drops were produced by mixing 1 µl reservoir solution with 1 µl protein solution. Diffraction-quality crystals were obtained after 1 d using a reservoir consisting of 0.2 *M* magnesium formate dihydrate pH 7.0, 20%(*w*/*v*) polyethylene glycol 3350. The protein solution consisted of protein at 14.5 mg ml^{-1}, as determined by measuring A_{280} using a NanoDrop spectrophotometer, in 100 m*M* ammonium acetate pH 7.2.

2.3. Data collection, structure determination and refinement

For data collection, crystals were harvested from the crystallization drop using a MiTeGen MicroMount (http://www.mitegen.com) and transferred for 10 s into a cryo-stabilization solution mimicking the mother liquor and supplemented with 18%(*w*/*v*) sucrose, 16%(*w*/*v*) glycerol, 16%(*w*/*v*) ethylene glycol, 4%(*w*/*v*) glucose. Cryoprotected crystals were mounted on CryoLoops, plunged into liquid nitrogen and placed in pucks for transfer and mounting at the synchrotron. Diffraction data were measured on beamline ID23-1 at the European Synchrotron Radiation Facility (ESRF), Grenoble, France using an ADSC Q315 detector and X-ray radiation of wavelength 0.9725 Å. The data were indexed and integrated with *DENZO* and scaled with *SCALEPACK* as implemented in *HKL*-2000 (v.0.98.704o;

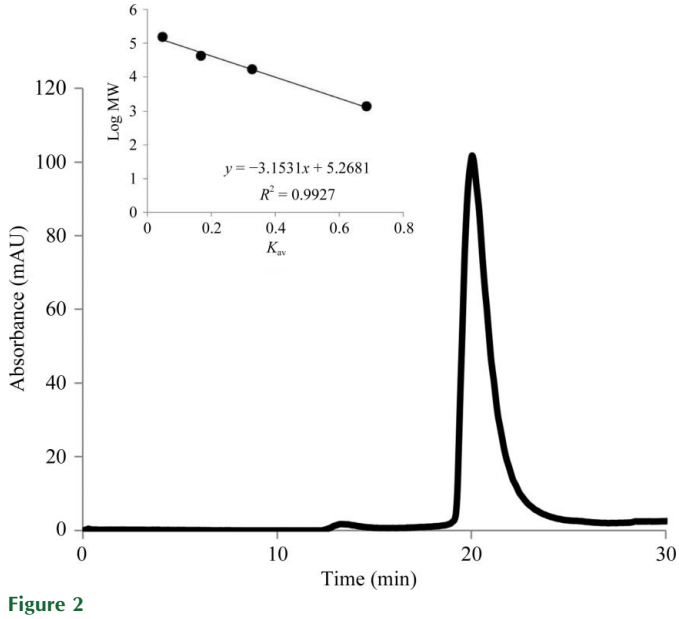

Figure 2
Purification of CA CTD by gel-filtration chromatography. The apparent molecular mass was calculated from the presented calibration curve (inset) using Bio-Rad Gel Filtration Standard (catalogue No. 151-1901). Since the protein was eluted after 20 min and the flow rate was 0.55 ml min^{-1}, the retention volume of the protein was 11 ml.

Table 1
X-ray data-collection and structure-refinement statistics for CA CTD.

Values in parentheses are for the highest resolution shell.

Resolution range (Å)	20.0–1.64 (1.67–1.64)
Space group	*P*1
Unit-cell parameters (Å, °)	a = 40.14, b = 43.58, c = 55.189, α = 74.02, β = 74.21, γ = 69.77
Total reflections	134659
Unique reflections	40722
Multiplicity	3.4 (2.1)
Completeness (%)	95.32 (78.24)
Mean $I/\sigma(I)$	22.6 (3.4)
Wilson B factor (Å^2)	11.58
R_{merge}	0.046 (0.333)
Reflections used in refinement	38632
R_{work}	0.1758 (0.1977)
R_{free}	0.2180 (0.2438)
No. of atoms	
Total	2997
Macromolecules	2632
Ligands	8
Water	347
No. of protein residues	330
R.m.s.d., bonds (Å)	0.006
R.m.s.d., angles (°)	1.07
Ramachandran favoured (%)	99
Ramachandran outliers (%)	0.3
Clashscore	3.61
Average B factors (Å^2)	
Overall	23.70
Macromolecules	22.80
Ligands	30.80
Solvent	29.90
PDB code	4ipy

Otwinowski & Minor, 1997). The structure was determined by molecular replacement (MR) in *MOLREP* (Vagin & Teplyakov, 2010) using the CA CTD structure (PDB entry 1a8o; Gamble *et al.*, 1997) as the initial model, yielding a convincing solution (correlation coefficient CC = 0.51) with four molecules in the asymmetric unit. The model was refined using iterative cycles of refinement in *PHENIX* (Adams *et al.*, 2010) and manual model rebuilding in *Coot* (Emsley *et al.*, 2010). Data-collection and refinement statistics are given in Table 1.

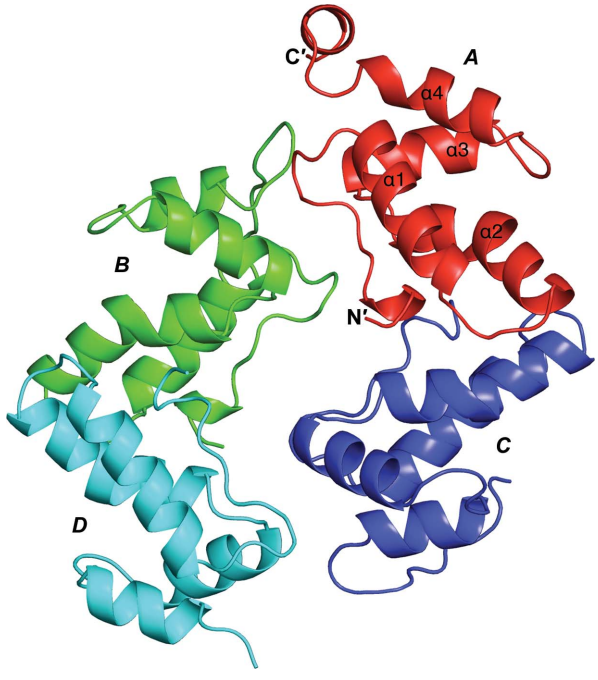

Figure 3
The asymmetric unit of CA CTD. Molecules *B* (green) and *D* (cyan) and molecules *A* (red) and *C* (blue) form canonical homodimers. The two homodimers are connected through contact between molecules *A* and *B*.

Table 2
R.m.s.d. values of C$^\alpha$ atoms for superposed structures.

The number of C$^\alpha$ atoms used in alignment is shown in parentheses. Values are in Å.

	4ipy			
Protein	Molecule *B*	Molecule *C*	Molecule *D*	1a80 (used for MR)
4ipy				
Molecule *A*	0.513 (66)	0.412 (68)	0.379 (67)	0.358 (52)
Molecule *B*	—	0.328 (66)	0.230 (53)	0.527 (51)
Molecule *C*	—	—	0.273 (65)	0.455 (52)
Molecule *D*	—	—	—	0.463 (52)

3. Results and discussion

3.1. Overview

The asymmetric part of the unit cell is composed of four CA CTD molecules (Fig. 3). Superposition of these molecules reveals that they are similar, with r.m.s.d. values ranging from 0.230 to 0.527 Å as measured for the C$^\alpha$ skeleton and as detailed in Table 2. The major differences between these crystallographically independent molecules were mostly concentrated in the region of the C-terminal tails. This region in molecule *A* (residues 221–231) is rotated by almost 180° compared with molecules *B* and *C*. In molecule *D* the C-terminal residues (222–231) are not detectable in the electron-density maps (lower ellipse in Supplementary Figure S1[1]).

Compared with the model used for molecular replacement (PDB entry 1a8o; Gamble *et al.*, 1997), the four molecules in the present structure exhibited low r.m.s.d. values (Table 2). The only significant difference between the model used for molecular replacement and the present structure was a relative movement of the loop between helices 1 and 2, with a maximal difference of 6 Å measured for the C$^\alpha$ skeleton (lower ellipse in Supplementary Fig. S1).

The four molecules in the present structure form distinct packing interfaces. Two of the largest interfaces are formed by molecules *B*–*C* and *A*–*D* [713 and 272 Å^2 as calculated using the *Protein Interfaces, Surfaces and Assemblies* service (*PISA*) at the European Bioinformatics Institute (http://www.ebi.ac.uk/pdbe/prot_int/pistart.html; Krissinel & Henrick, 2007); Supplementary Table S1]. Each of these interfaces participates in an 'infinite' heterologous association (Monod *et al.*, 1965), which geometrically resembles two infinite fibres of crystallographically independent molecules (Supplementary Fig. S2). These fibres form additional interfaces which consist of a pair of canonical dimers *A*–*C* and *B*–*D* (Fig. 3) linked by the interface between the N-terminal and the C-terminal domains of molecules *A* and *B*, respectively (Fig. 4). In each dimer the molecules are connected through a large interface (506 Å^2) which resembles the previously characterized CA dimerization interface (Gamble *et al.*, 1997; Berthet-Colominas *et al.*, 1999; Ternois *et al.*, 2005; Ivanov *et al.*, 2007; Worthylake *et al.*, 1999) and is formed by the mutual packing of helix 2 from the neighbouring molecules *A*–*C* and *B*–*D* (Fig. 3).

3.2. The Arg154, Lys158, Pro157 and Arg167 residues of the MHR participate in interface formation

It has been hypothesized that the MHR of HIV-1 and of other retroviruses mediates Gag–Gag interactions during the assembly of

[1] Supplementary material has been deposited in the IUCr electronic archive (Reference: TT5039).

the immature particle (Mammano *et al.*, 1994; Orlinsky *et al.*, 1996; Chang *et al.*, 2007; Ganser-Pornillos *et al.*, 2004; von Schwedler *et al.*, 2003). However, the structural mechanism by which this region participates in the assembly of Gag is not known.

The structure of the CA CTD after deletion of a single amino acid (Ivanov *et al.*, 2007) reveals domain swapping between two molecules of the asymmetric unit, resulting in a dimeric assembly. This intriguing assembly was shown to be mediated mainly through interactions of MHR residues. It was therefore proposed that the 'domain-swapped' dimer serves as an intermediate assembly in the formation of the immature Gag lattice.

The present structure revealed a new CTD interface that associates two pairs of CA CTD molecules (dimers *A*–*C* and *B*–*D*; Fig. 3). This new interface incorporates the following four conserved MHR residues.

(i) Arg154. The main-chain O atom of Arg154 (molecule *A*; Fig. 4) forms a hydrogen bond to Asp197 OD2 (molecule *B*; Fig. 4). Both truncation and an Arg154Ala mutation prevent CA from forming dimers *in vitro* (del Alamo *et al.*, 2003).

(ii) Lys158. Lys158 from molecule *A* forms hydrogen bonds to the main-chain carbonyl O atoms of three different residues from molecule *B*: Thr216, located in helix 4, and Gln219 and Gly220, which are both located in the adjacent loop (Fig. 4). The ε-amine group of Lys158 from molecule *B* forms a hydrogen bond to the OD1 atom of Asn193, which is located in helix 2 of molecule *A* (Fig. 4). Several mutagenesis studies have indicated that the Lys158Ala mutation, together with Lys158Asp or Lys158Gln, markedly impairs Gag assembly, significantly diminishes the presence of conical capsids and completely abolishes infectivity (Ganser-Pornillos *et al.*, 2004; von Schwedler *et al.*, 2003; Chang *et al.*, 2007). Notably, Gln219, which forms an intermolecular hydrogen bond to Lys158, also participates in the intermolecular interactions of the NTD–CTD interface in the mature capsid lattice (Pornillos *et al.*, 2009), and mutagenesis of Gln219 impairs both capsid core stability *in vivo* and infectivity (Forshey *et al.*, 2002; von Schwedler *et al.*, 2003). In addition, a recent NMR solution structure (Byeon *et al.*, 2009) revealed that Gln219 participates in an alternative CTD–CTD interface in tubular assemblies of CA. This interface is mediated through interactions between helix 3 of one CTD and helix 4 of the neighbouring CTD.

(iii) Pro157 (molecule *A*; Fig. 4). This amino acid forms hydrophobic interactions with Ile201, which is located in helix 3 (molecule *B*; Fig. 4). Despite the relative conservation of Pro157, there is no evidence that this residue mediates the formation of either the immature or the mature particle.

(iv) Arg167 (molecule *A*; Fig. 4). Electrostatic interactions of Arg167 with Asp197 (molecule *B*; Fig. 4) stabilize the tertiary structure of CA CTD by adhering the MHR to helix 2 (Gamble *et al.*, 1997). The Arg167Ala mutation leads to a threefold decrease in virus-particle yield and results in the formation of aberrant cores only (Mammano *et al.*, 1994).

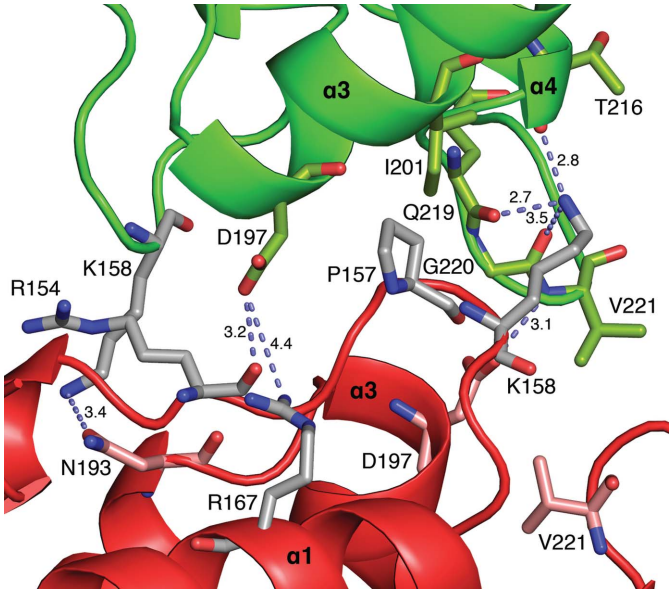

Figure 4
Cartoon view of the new interface which is formed by interactions between molecules *A* (red) and *B* (green). Side chains of important interface residues are shown as sticks and the conserved MHR residues Arg154, Pro157, Lys158 and Arg167 are coloured grey. The hydrogen-bonding network and the ionic interaction are shown as blue dashed lines.

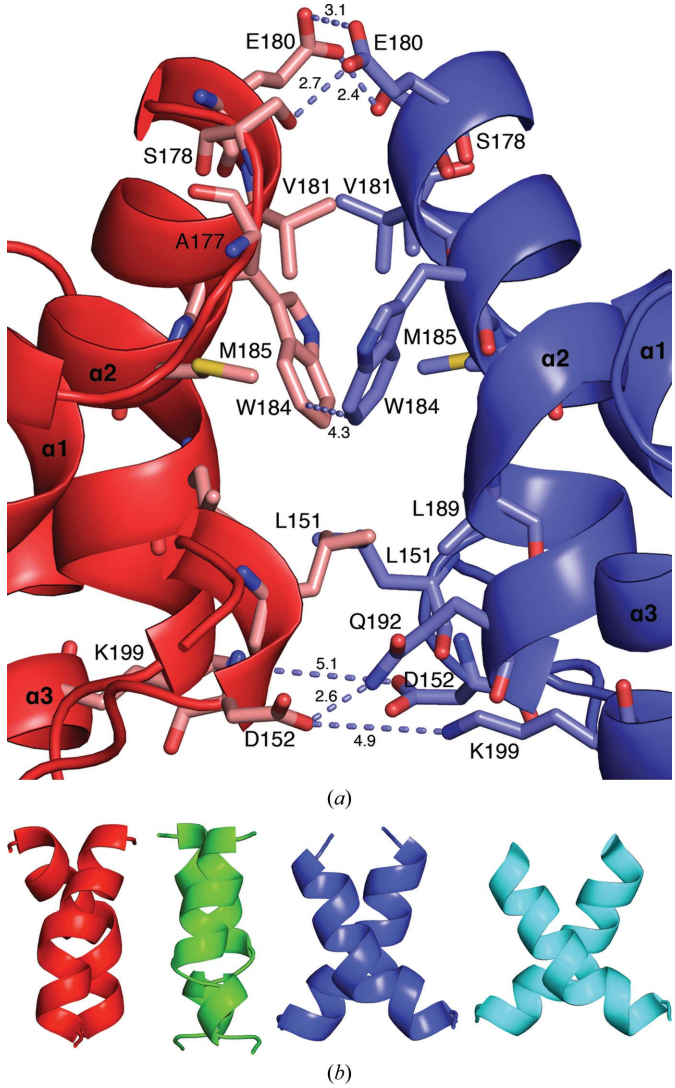

Figure 5
Cartoon view of the CA CTD canonical dimerization interface. (*a*) The CTD–CTD dimerization interface is formed by the parallel packing of helix 2 of two CTD molecules (molecules *A* and *C* as presented in Fig. 2). Side chains of key interface residues are shown as sticks, the aromatic interaction between Trp184 residues is shown as a blue dotted line and the hydrogen-bonding network and ionic interactions are shown as in Fig. 3. (*b*) View of the different crossing angles of the helix 2 pairs in the present structure (red) and in PDB entries 1a43 (green), 1a8o (purple) and 2bou (cyan).

To the best of our knowledge, this is the first report to suggest that these four conserved MHR residues (Arg154, Pro157, Lys158 and Arg167) participate in intermolecular CTD–CTD interactions. As described above, Asp197 of molecule *B* interacts with two MHR residues: Arg154 and Arg167. In addition, the OD2 atom of Asp197 in molecule *A* forms a hydrogen bond to the main-chain N atom of Val221 in molecule *B*. Mutation of Asp197 severely damages *in vivo* assembly of Gag and CA and suppresses infectivity (von Schwedler *et al.*, 2003; Ganser-Pornillos *et al.*, 2004).

3.3. CTD dimerization interface

The CTD–CTD dimerization interfaces inferred from our crystal structure are formed *via* the mutual packing of helix 2 from each CA CTD molecule to helix 2 of its symmetry-related molecule (Fig. 5*a*). Trp184 and Met185, which are important both for capsid core formation and for Gag multimerization (Gamble *et al.*, 1997; von Schwedler *et al.*, 2003; Burniston *et al.*, 1999; the latter was deduced from mutagenesis studies but with no supporting structural data), are buried in the hydrophobic core at each interface in the present model. In addition, helix 2 of the model structure clearly shows a kink, which has also been found in most previously reported structures of CA CTD (Gamble *et al.*, 1997; Ternois *et al.*, 2005; Berthet-Colominas *et al.*, 1999; Worthylake *et al.*, 1999).

In general, the dimerization interface resembles the CTD–CTD interface in the crystallographic structures of CA CTD mentioned earlier. However, as shown in Fig. 4(*b*), the crossing angles of helix 2 vary between the structures. This geometric diversity is a result of different interactions between different interface residues among the structures. The packing geometry of helix 2 in the present structure most resembles that of the structure with PDB code 1a43 (Worthylake *et al.*, 1999), with an r.m.s.d. on C^{α} atoms of 3.14 Å (Fig. 5*b*). We analyzed and compared the key interactions in the present structure and in PDB entry 1a43. Among other differences, Leu151 in the present crystal forms three different hydrophobic interactions with Trp184 and Leu151 of the neighbouring CTD and forms a reciprocal hydrophobic interaction with Leu189 (Fig. 5*a*). In contrast, in the 1a43 structure Leu151 interacts with Thr188, Val191 and Gln192 (Worthylake *et al.*, 1999). Furthermore, Trp184 in the present structure forms both hydrophobic and aromatic interactions with the symmetry-related Trp184 (Fig. 56), whereas in PDB entry 1a43 the neighbouring Trp184 residues do not form contact interactions (Worthylake *et al.*, 1999).

In conclusion, we have determined the high-resolution crystal structure of HIV-1 CA CTD. The crystal lattice is composed of two connected canonical CA CTD dimers. The interface connecting the CTD dimers consists of the four conserved MHR residues Arg154, Pro157, Lys158 and Arg167. Previous mutagenesis studies have revealed that Lys158 and two other interface residues, Gln219 and Asp197, mediate assembly of the immature and the mature particle (von Schwedler *et al.*, 2003; Ganser-Pornillos *et al.*, 2004; Chang *et al.*, 2007; Forshey *et al.*, 2002). Consistent with these previous studies and based on the present structure, we contemplate that our newly determined interface forms an intermediate assembly during organization of the immature particle. Therefore, we suggest that interference with this interface may inhibit the formation of virus particles and thus may serve as an efficient therapeutic way to combat HIV.

We are grateful to W. I. Sundquist for the HIV-1 CA CTD plasmid construct. We thank the ESRF, Grenoble, France for use of the macromolecular crystallographic data-collection facilities and the ID14-4 staff for their assistance.

References

Adams, P. D. *et al.* (2010). *Acta Cryst.* D**66**, 213–221.
Adamson, C. S. & Jones, I. M. (2004). *Rev. Med. Virol.* **14**, 107–121.
Alamo, M. del, Neira, J. L. & Mateu, M. G. (2003). *J. Biol. Chem.* **278**, 27923–27929.
Berthet-Colominas, C., Monaco, S., Novelli, A., Sibaï, G., Mallet, F. & Cusack, S. (1999). *EMBO J.* **18**, 1124–1136.
Borsetti, A., Ohagen, A. & Göttlinger, H. G. (1998). *J. Virol.* **72**, 9313–9317.
Burniston, M. T., Cimarelli, A., Colgan, J., Curtis, S. P. & Luban, J. (1999). *J. Virol.* **73**, 8527–8540.
Byeon, I.-J. L., Meng, X., Jung, J., Zhao, G., Yang, R., Ahn, J., Shi, J., Concel, J., Aiken, C., Zhang, P. & Gronenborn, A. M. (2009). *Cell*, **139**, 780–790.
Chang, Y.-F., Wang, S.-M., Huang, K.-J. & Wang, C.-T. (2007). *J. Mol. Biol.* **370**, 585–597.
Emsley, P., Lohkamp, B., Scott, W. G. & Cowtan, K. (2010). *Acta Cryst.* D**66**, 486–501.
Forshey, B. M., von Schwedler, U., Sundquist, W. I. & Aiken, C. (2002). *J. Virol.* **76**, 5667–5677.
Gamble, T. R., Vajdos, F. F., Yoo, S., Worthylake, D. K., Houseweart, M., Sundquist, W. I. & Hill, C. P. (1996). *Cell*, **87**, 1285–1294.
Gamble, T. R., Yoo, S., Vajdos, F. F., von Schwedler, U. K., Worthylake, D. K., Wang, H., McCutcheon, J. P., Sundquist, W. I. & Hill, C. P. (1997). *Science*, **278**, 849–853.
Ganser-Pornillos, B. K., Cheng, A. & Yeager, M. (2007). *Cell*, **131**, 70–79.
Ganser-Pornillos, B. K., von Schwedler, U. K., Stray, K. M., Aiken, C. & Sundquist, W. I. (2004). *J. Virol.* **78**, 2545–2552.
Gitti, R. K., Lee, B. M., Walker, J., Summers, M. F., Yoo, S. & Sundquist, W. I. (1996). *Science*, **273**, 231–235.
Göttlinger, H. G. (2001). *AIDS*, **15**, Suppl. 5, S13–S20.
Ivanov, D., Tsodikov, O. V., Kasanov, J., Ellenberger, T., Wagner, G. & Collins, T. (2007). *Proc. Natl Acad. Sci. USA*, **104**, 4353–4358.
Kelly, B. N., Howard, B. R., Wang, H., Robinson, H., Sundquist, W. I. & Hill, C. P. (2006). *Biochemistry*, **45**, 11257–11266.
Krissinel, E. & Henrick, K. (2007). *J. Mol. Biol.* **372**, 774–797.
Lanman, J., Lam, T. T., Barnes, S., Sakalian, M., Emmett, M. R., Marshall, A. G. & Prevelige, P. E. Jr (2003). *J. Mol. Biol.* **325**, 759–772.
Lanman, J., Lam, T. T., Emmett, M. R., Marshall, A. G., Sakalian, M. & Prevelige, P. E. Jr (2004). *Nature Struct. Mol. Biol.* **11**, 676–677.
Larkin, M. A., Blackshields, G., Brown, N. P., Chenna, R., McGettigan, P. A., McWilliam, H., Valentin, F., Wallace, I. M., Wilm, A., Lopez, R., Thompson, J. D., Gibson, T. J. & Higgins, D. G. (2007). *Bioinformatics*, **23**, 2947–2948.
Li, S., Hill, C. P., Sundquist, W. I. & Finch, J. T. (2000). *Nature (London)*, **407**, 409–413.
Mammano, F., Ohagen, A., Höglund, S. & Göttlinger, H. G. (1994). *J. Virol.* **68**, 4927–4936.
McPherson, A. (1982). *Preparation and Analysis of Protein Crystals*, 1st ed. New York: Wiley.
Momany, C., Kovari, L. C., Prongay, A. J., Keller, W., Gitti, R. K., Lee, B. M., Gorbalenya, A. E., Tong, L., McClure, J., Ehrlich, L. S., Summers, M. F., Carter, C. & Rossmann, M. G. (1996). *Nature Struct. Biol.* **3**, 763–770.
Monod, J., Wyman, J. & Changeux, J.-P. (1965). *J. Mol. Biol.* **12**, 88–118.
Orlinsky, K. J., Gu, J., Hoyt, M., Sandmeyer, S. & Menees, T. M. (1996). *J. Virol.* **70**, 3440–3448.
Otwinowski, Z. & Minor, W. (1997). *Methods Enzymol.* **276**, 307–326.
Pornillos, O., Ganser-Pornillos, B. K., Kelly, B. N., Hua, Y., Whitby, F. G., Stout, C. D., Sundquist, W. I., Hill, C. P. & Yeager, M. (2009). *Cell*, **137**, 1282–1292.
Scarlata, S. & Carter, C. (2003). *Biochim. Biophys. Acta*, **1614**, 62–72.
Schwedler, U. K. von, Stray, K. M., Garrus, J. E. & Sundquist, W. I. (2003). *J. Virol.* **77**, 5439–5450.
Tang, C., Ndassa, Y. & Summers, M. F. (2002). *Nature Struct. Biol.* **9**, 537–543.
Ternois, F., Sticht, J., Duquerroy, S., Kräusslich, H.-G. & Rey, F. A. (2005). *Nature Struct. Mol. Biol.* **12**, 678–682.
Vagin, A. & Teplyakov, A. (2010). *Acta Cryst.* D**66**, 22–25.
Wong, H. C., Shin, R. & Krishna, N. R. (2008). *Biochemistry*, **47**, 2289–2297.
Worthylake, D. K., Wang, H., Yoo, S., Sundquist, W. I. & Hill, C. P. (1999). *Acta Cryst.* D**55**, 85–92.